Spatially Resolved Characteristics and Analytical Modeling of Elastic Non-Newtonian Secondary Breakup

Sharon E. Snyder, Paul E. Sojka[1*]
Department of Mechanical Engineering
Purdue University, West Lafayette, IN USA
snyder22@purdue.edu, sojka@ecn.purdue.edu

Abstract

The secondary breakup of elastic non-Newtonian liquid drops was investigated experimentally to determine fragment size and velocity distributions. Xanthan gum – water solutions of various concentrations ranging from 0.1% to 1.0% by weight were prepared and injected into a high speed air stream. PIV techniques were employed to characterize the air stream velocity. The fragment size and velocity distributions of fragments resulting from secondary atomization were characterized using a dual-PDA system. The primary focus is on the bag breakup regime. An analytical model for drop initiation time was developed and predictions compared to experimental data.

Introduction

Newtonian liquid breakup is characterized by a morphology consisting of the following regimes for low *Oh*: vibrational, bag, multimode, sheet-thinning, and catastrophic. Each regime differs qualitatively from the others and produces different fragment sizes. In addition, each regime has several important dimensionless times. Of importance are correlations for both the initiation time, T_{ini}, and the total breakup time, T_{tot}. Analytical models that predict the breakup process are of interest.

Developing a detailed model of a spray is a difficult process due to the complexity of events that occur. Droplet deformation is one process during the overall atomization process, with droplet drag and breakup also of importance, especially in spray combustion. Several models have been proposed and used to predict deformation and breakup, with the most commonly being the TAB [1], DDB [2], and improved TAB (I-TAB) [3] versions. They only predict drop deformation and oscillation, mainly because of the simplicity of the governing physics of these processes, but also because it is the first step for each breakup mode. Currently, there is a lack of analytical models that accurately describe all the modes of secondary atomization.

Only a few studies have focused on non-Newtonian drop breakup. While the breakup mechanisms observed are similar to those seen for Newtonian drops, there is still not enough data to determine common characteristics or processes for non-Newtonian secondary breakup. The same types of physical mechanisms are responsible for secondary breakup, but the way in which non-Newtonian drops resist deformation and breakup is different due to their complex rheological properties. This leads to different characteristics that mark each breakup mode. The current analytical models used for Newtonian drops are not necessarily appropriate for non-Newtonian drops.

Following the work of Bartz *et al.* [7] and Flock [11], PDA measurements were taken to determine fragment size and velocity distributions of the secondary atomization process. Knowledge of these parameters will help with the design and/or optimization of technical systems such as gas turbine combustors or film coating processes. The fragment size and velocity distributions in the wake region of the fragmenting drop will be plotted against appropriate dimensionless groups to illustrate how the two distributions change with respect to these parameters. Previous work on fragments from secondary breakup has mainly studied fragment sizes, not velocities. As an example, work by Villermaux and Bossa [8] was focused on the distribution of fragment sizes, and the end result was a plot of drop size distribution versus initial drop diameter. Here we report both size and velocity distributions.

Numerical and/or Experimental Methods

The TAB model is based on an analogy between an oscillating and distorting droplet and a spring-mass-damper system. In this analogy, the spring force is equivalent to the surface tension, the driving force is equivalent to the external aerodynamic load, and the damping force is equivalent to the liquid viscosity:

$$m\ddot{x} = F - kx - \Gamma\dot{x} \qquad [1]$$

Here m is the mass of the drop, x is the displacement of the equator of the drop from its equilibrium position, F is the external aerodynamic force, k is the spring constant, and Γ is the viscous damping coefficient.

Following Taylor's analogy, the coefficients in Equation 1 are defined as:

* Corresponding author: sojka@ecn.purdue.edu

$$\frac{F}{m} = C_F \frac{\rho_g u^2}{\rho_d r_0} \quad [2]$$

$$\frac{k}{m} = C_k \frac{\sigma}{\rho_d r_0^3} \quad [3]$$

$$\frac{\Gamma}{m} = C_d \frac{\mu_d}{\rho_d r_0^2} \quad [4]$$

where r_0 is the initial spherical drop radius, and C_F, C_k, and C_d are dimensionless constants equal to 1/3, 8, and 5, respectively, for Newtonian liquids. O'Rourke and Amsden [1] used these constants, initially computed by Lamb [4] who considered only the fundamental mode of oscillation. As López [5] notes, this is a shortcoming of the model because there are various modes. Despite this, the TAB model will still be used here since the fundamental mode is assumed to be a good approximation of the observed deformation of drops.

The breakup condition for the TAB model is $x > C_b r_0$, where C_b is an additional dimensionless constant equal to ½. By defining the dimensionless displacement of the drop equator y as $y = x/ C_b r_0$, we can non-dimensionalize x. Park *et al.* [3] used a modified form of this expression and assumed a dimensionless time $t^* = tV_{rel}/r_0$ to obtain the following equation in terms of dimensionless groups:

$$\ddot{y} = \frac{2}{3\varepsilon} - \frac{8}{We\varepsilon} y - \frac{5N}{\mathrm{Re}\,\varepsilon} \dot{y} \quad [6]$$

where

$$\varepsilon = \frac{\rho_d}{\rho_g} \quad [7]$$

$$We = \frac{\rho_d V_{rel}^2 r_0}{\sigma} \quad [8]$$

$$N = \frac{\mu_d}{\mu} \quad [9]$$

$$Re = \frac{\rho_g V_{rel} r_0}{\mu} \quad [10]$$

In order to develop a non-Newtonian version of this model, the rheological parameters that distinguish viscoelastic non-Newtonian drop from Newtonian ones have to be taken into consideration. As a result, four main aspects were incorporated into the viscoelastic TAB model.

First, the constant Newtonian shear viscosity μ in the $\dot{y}$ term of Equation 5 was replaced by a power-law effective viscosity μ_{eff} to account for the shear-thinning behavior of the XG-water solutions. It should be noted that the power-law model only accounts for the inelastic part of the liquid rheology. (The elastic portion is covered by another term to be discussed later.) The relevant expression for μ_{eff} is:

$$\mu_{eff} = K\dot{\gamma}^{n-1} \quad [11]$$

where the strain rate $\dot{\gamma}$ is approximated as:

$$\dot{\gamma} = \frac{V_{rel}}{2r_0} \quad [12]$$

Second, the viscoelastic non-Newtonian version of the model included the time dependence of drop velocity, U_d, since it is not constant and influences the effective viscosity through the applied shear. The expression for time dependent drop velocity was obtained from the equation of drop motion with $C_{D,sphere} = 0.44$ (since Re was greater than 500 for all experiments). U_d was obtained by integrating using a 4th order Runge-Kutta routine.

Third, the deformation of the drop radius was considered. Finally, the viscoelastic nature of the solutions was considered. This was accomplished by using a Maxwell model, composed of a purely viscous damper, representing the solution viscosity, and a purely elastic (Hookean) spring. The latter represents the solution elasticity:

$$\frac{1}{E}\dot{\tau} + \frac{\tau}{\mu} = \dot{\gamma} \quad [13]$$

where τ is the shear stress and E is the elastic modulus. If we rewrite Equation 3 to solve for τ, we find that the relaxation time, λ, can be expressed as $\lambda = \mu/E$. Note that the spring force is proportional to the displacement, so this proportionality constant must be a type of spring constant:

$$F = EA_{cross-section}\frac{\Delta L}{L} \quad [14]$$

where L is taken to be r and ΔL to be x. We must also take into account the volume and area of the deformed drop. Adding this spring constant to the x term in Equation 1 gives the form of the viscoelastic non-Newtonian TAB model. After rearrangement and substitution, we have an ODE for viscoelastic drop deformation:

$$\ddot{y} = \frac{2}{3\varepsilon} - \frac{8}{We\varepsilon}\left(1 + c\frac{\sigma\lambda}{R\mu_d}\right)y - \frac{5N}{Re\varepsilon}\dot{y} \quad [15]$$

where:

$$\varepsilon = \frac{\rho_d}{\rho_g} \quad [16]$$

$$We = \frac{\rho_d \left(U - U_d\right)^2 R}{\sigma} \quad [17]$$

$$Re = \frac{\rho_g \left(U - U_d\right) R}{\mu} \quad [18]$$

$$N = \frac{\mu_{eff}}{\mu} \quad [19]$$

μ_{eff} is defined in Equation 11 and $\dot{\gamma}$ in Equation 12, and c is a relaxation time-dependent constant.

The three equation system is solved using a 4th order Runge-Kutta routine. Inputs are the drop physical properties (ρ_d, σ, K, n, λ), drop diameter, and drop environment (gas velocity, ambient viscosity). The outputs of interest are the deformed drop radius and dimensionless displacement as functions of time. The deformed drop radius is reported as the magnitude when $t=T_{ini}$.

Elastic non-Newtonian drop breakup morphology and breakup times were obtained for drops composed of xanthan gum (XG)–water solutions that were exposed to high speed air flows. The main experimental components are the air flow system, the liquid flow system plus droplet generator, and the dual-PDA system (Dantec Dynamics GmbH, Germany). Both PIV and LDA techniques were employed to characterize the air stream velocity with good agreement between the two sets of measurements. Single xanthan gum droplets were injected downwards at a location downstream of the air nozzle. Single droplets were injected instead of a steady stream or droplet chain to avoid droplet interaction. Droplet size and velocity distributions were measured using the PDA system. For this case, we investigated water and 0.1, 0.2, and 0.3 wt-% XG solutions.

Results and Discussion

Predicted T_{ini} is plotted against We, as shown in Figures 1 – 5. Here, K varies from 0.19 to 2.79. Note that T_{ini} increases with K, as expected, since increasing K increases the resistive force via an increase in the effective viscosity. Predictions for the 0.1% solution are approximately 30% larger at small We. The model underpredicts initiation time at high We for the 0.5% solution by approximately 20%. For both the 0.7% and 1.0% solutions, the model consistently underpredicts T_{ini} by about 20% for the 0.7% solution and 30% for the 1.0% solution. The differences could be due to the drop drag model used ([6], [10]) or to the condition for breakup that was considered.

Additional changes to the original TAB model [1] may be made to the dimensionless constants C_F, C_k, and C_d, since the values used are those Lamb [4] calculated for the purely viscous case. Another modeling option is to extend the work done by Villermaux and Bossa [8]. Future work includes modifying the axisymmetric Euler equation to include viscous effects. This change will result in a modification to the equation for the pressure difference between the center of the drop and its rim (Equation 8 in [8]).

Work has already been done to adapt the work of Villermaux and Bossa [8] to the Newtonian bag breakup regime by Kulkarni [9]. Here we will extend the efforts of [8] and [9] to the initial deformation of viscous non-Newtonian liquid drops.

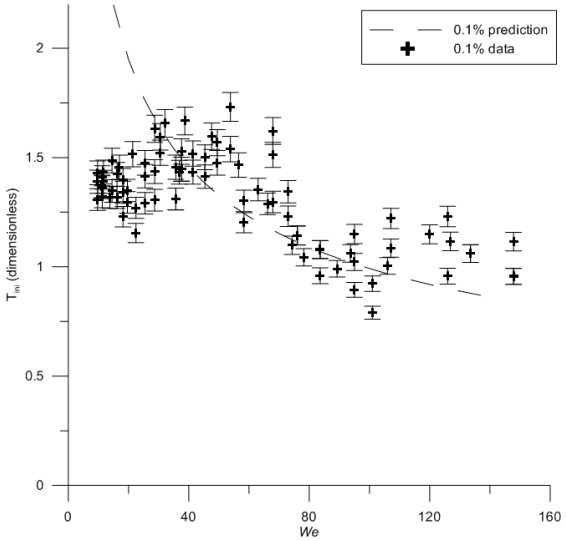

Figure 1. Experimental and predicted initiation times (T_{ini}) versus *We*, 0.1% XG

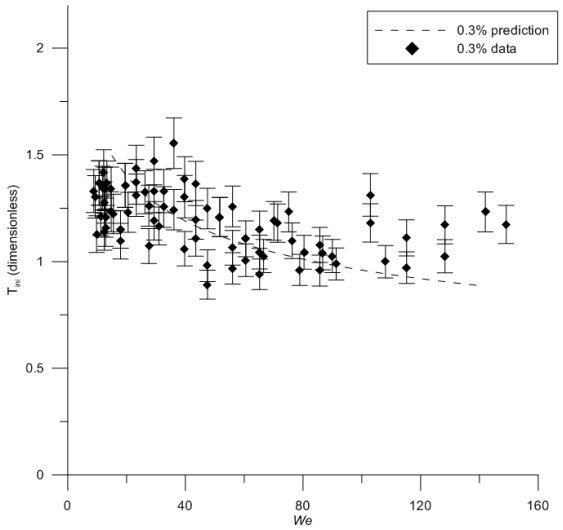

Figure 2. Experimental and predicted initiation times (T_{ini}) versus *We*, 0.3% XG

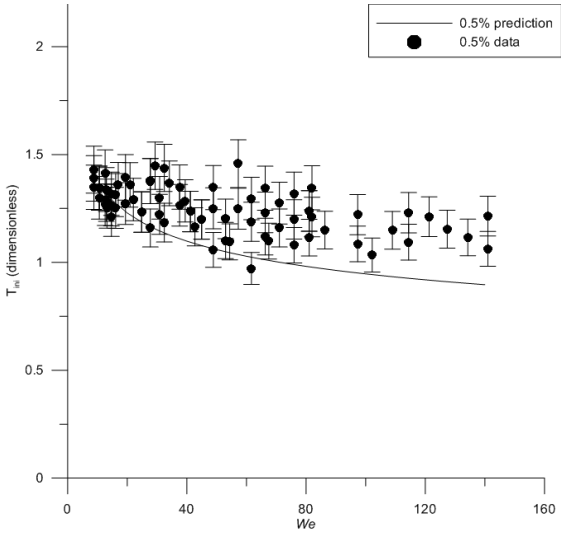

Figure 3. Experimental and predicted initiation times (T_{ini}) versus *We*, 0.5% XG

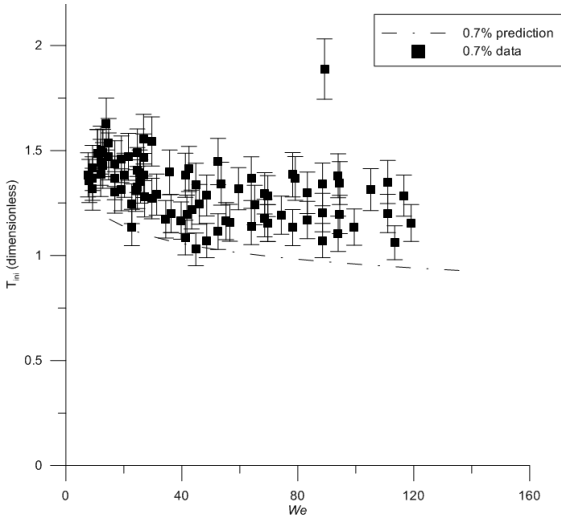

Figure 4. Experimental and predicted initiation times (T_{ini}) versus *We*, 0.7% XG

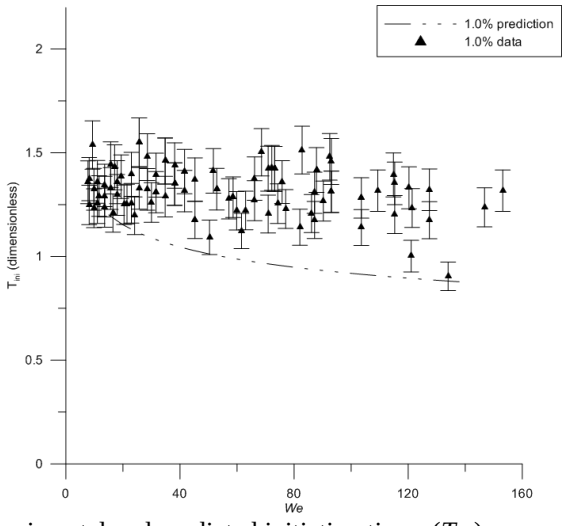

Figure 5. Experimental and predicted initiation times (T_{ini}) versus *We*, 1.0% XG

Measured fragment size distributions (for the bag breakup regime) are shown in Figures 6 – 12. The sample size for 0.1 wt-% XG was approximately 17 000, 0.3 wt-% XG was approximately 3 000, and 0.5 wt-% XG was approximately 1 600.

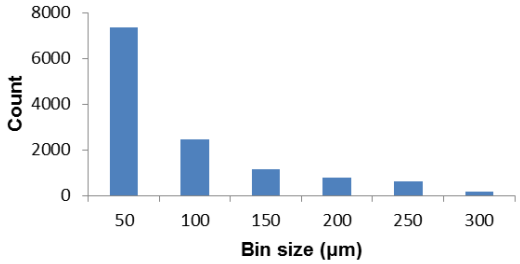

Figure 6. 0.1%, *We* = 14.5

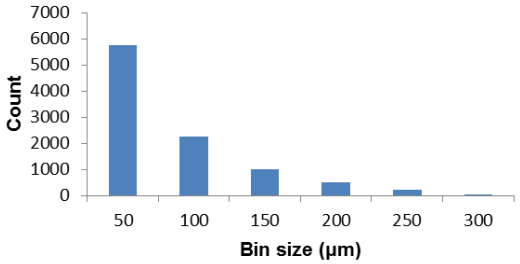

Figure 7. 0.1%, *We* = 16

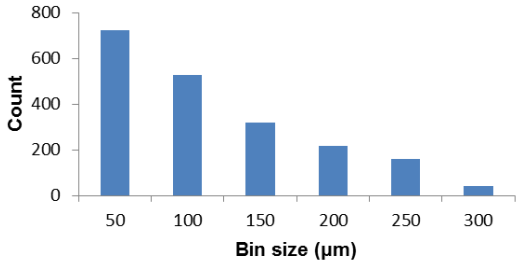

Figure 8. 0.2%, *We* = 14.5

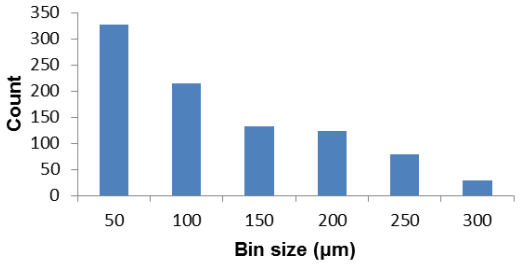

Figure 9. 0.2%, *We* = 18

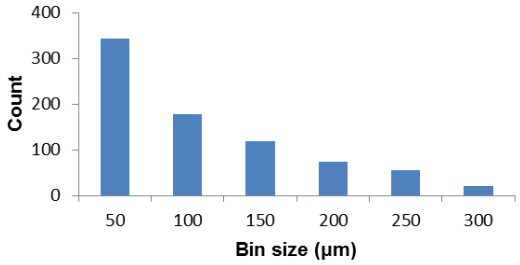

Figure 10. 0.3%, *We* = 13

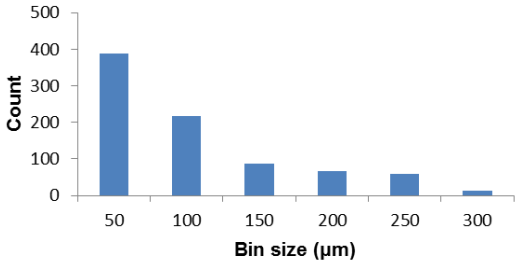

Figure 11. 0.3%, *We* = 15

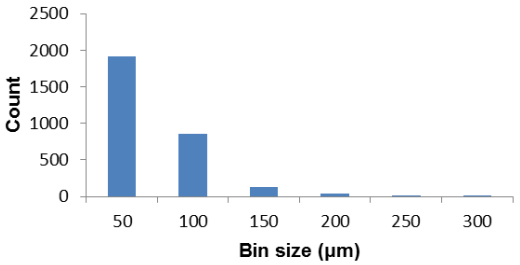

Figure 12. DI water, *We* = 20

Note the disparity between the two distributions. As might be expected, the viscoelastic liquid produces fragments having noticeably larger sizes (250 and 300 µm) and the corresponding bin occupancies are considerably greater.

Measured fragment velocity distributions for xanthan gum solutions are shown Figures 13 – 15.

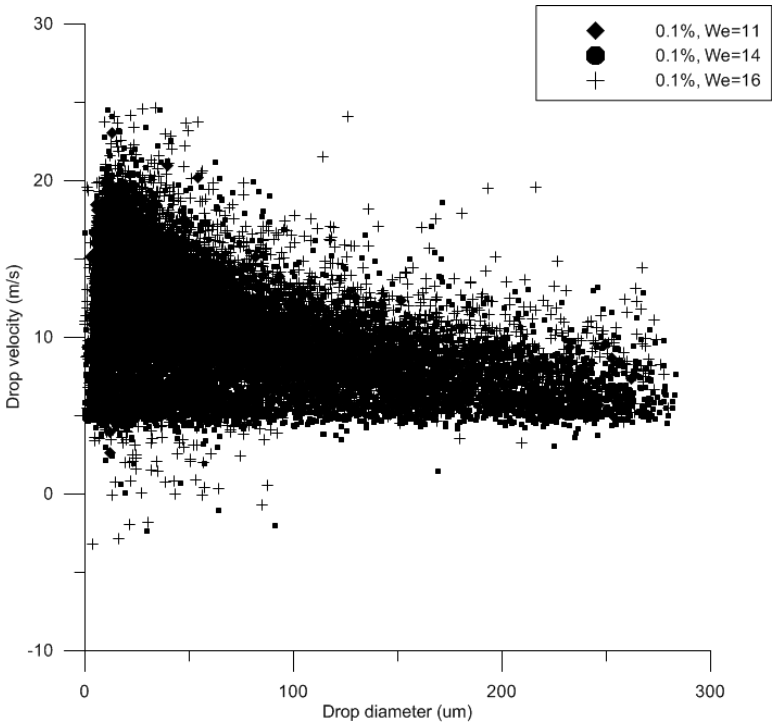

Figure 13. 0.1% XG at *We* = 11.5, 14.5, and 16

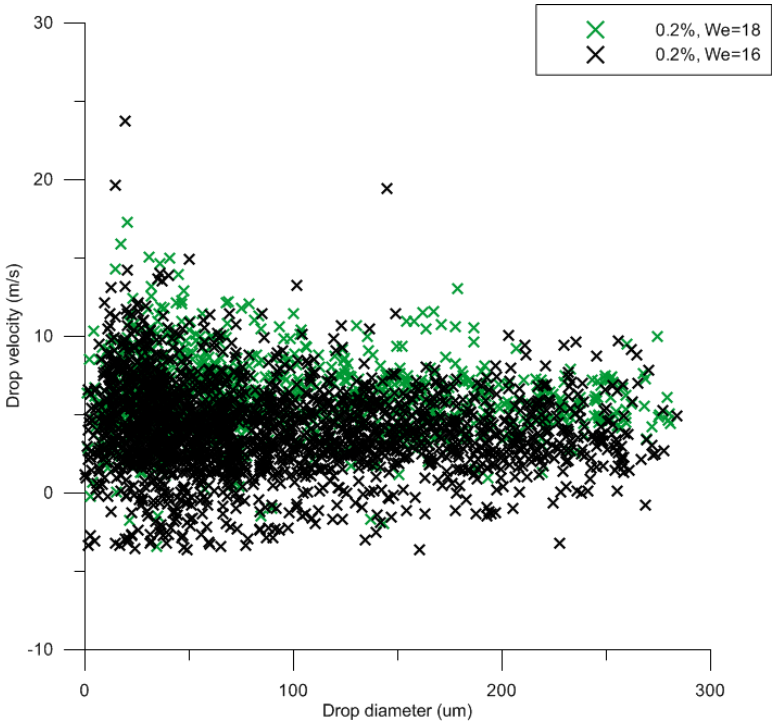

Figure 14. 0.2% XG at *We* = 14.5 and 18

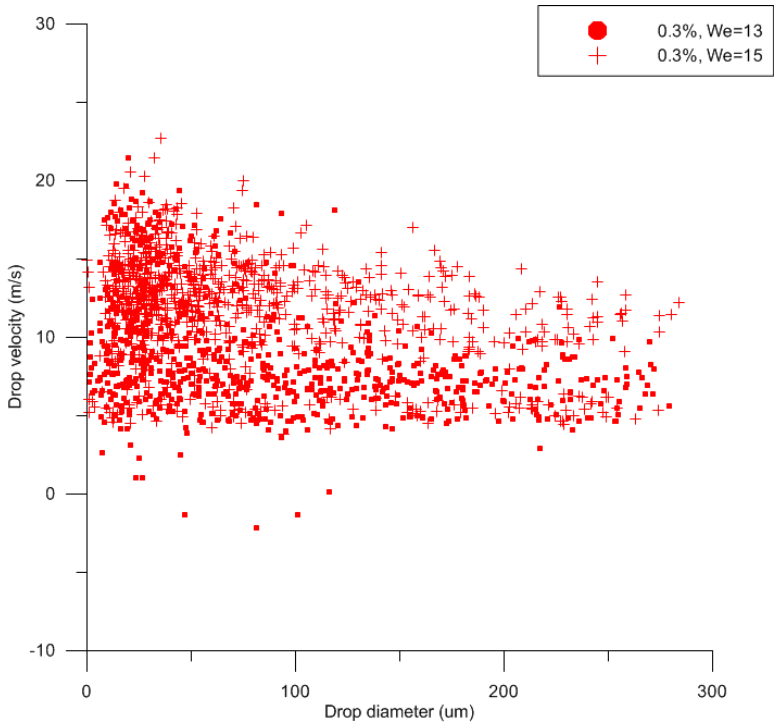

Figure 15. 0.3% XG at *We* = 13 and 15

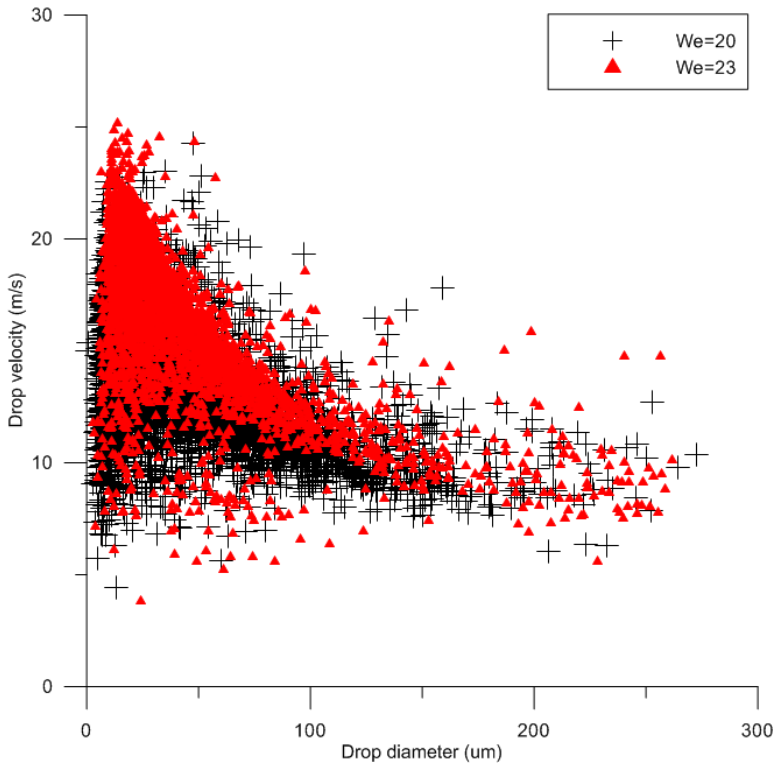

Figure 16. DI water at *We* = 20 and 23

Summary and Conclusions

A new TAB-based droplet deformation model was developed that included viscoelastic rheological effects. It did reasonable job of predicting the influence of liquid rheology on initial drop deformation. Improvements may still be made by choice of a different droplet drag model, or by adjusting breakup conditions.

Experimental data for viscoelastic fragment sizes and velocity distributions were presented and compared to water data. The viscoelastic fragments were greater in size and had a larger fraction of bigger fragments. Fragment velocity distributions differed in terms of the range of drop velocities and the number of drop diameters at a given velocity.

To obtain a better understanding of elastic non-Newtonian secondary breakup, some aspects of drop morphology and breakup times still need to be studied. First, the influence of elastic liquid rheology on breakup morphology should be studied in more depth by using different XG-water solutions or using other elastic non-Newtonian solutions. Lower *n* values and higher *K* values could be achieved. This will allow for comparison between present results and with those reported in other studies. Also, the rheological model used for μ_{eff} should be examined and alternate effective viscosity equations considered. Future improvements of the deformation based model could include an improved description of droplet deformation and drag during fragmentation, as well as improved fragment starting conditions.

Acknowledgements

Supported by U.S. Army Research Office – MURI Grant W911NF-08-1-0171

Reference

[1] O'Rourke, P.J., and Amsden, A.A. (1987). The TAB method for numerical calculation of spray droplet breakup. In: *International Fuels and Lubricants Meeting and Exposition*, Toronto, Ontario, November 2-5.

[2] Ibrahim, E.A., Yang, H.Q., and Przekwas, A.J. (1993). Modeling of spray droplets deformation and breakup. *Journal of Propulsion*, 9 (4), 651-654.

[3] Park, J.H., Yoon, Y., and Hwang, S.S. (2002). Improved TAB model for prediction of spray droplet deformation and breakup. *Atomization and Sprays*, 12 (4), 387-401.

[4] Lamb, H. (1932). *Hydrodynamics* (6th ed.). New York: Dover.

[5] López Rivera, C. (2010). *Secondary atomization of inelastic non-Newtonian liquid drops*. Thesis (PhD). West Lafayette: Purdue University.

[6] Liu, A.B., and Reitz, R.D. (1993). Mechanisms of air-assisted liquid atomization. *Atomization and Sprays*, 3 (1), 55-75.

[7] Bartz, Frank-Oliver, *et al*. (2011). "Comparison of droplet breakup models for single droplet fragmentation under varying accelerations." *ILASS – Europe 2011, 24th European Conference on Liquid Atomization and Spray Systems, Estoril, Portugal*. September, 2011.

[8] Villermaux, E., and B. Bossa. (2009). "Single-drop fragmentation determines size distribution of raindrops." Nature Physics, 5, p. 697 – 702.

[9] Kulkarni, V. (2012). "Secondary Atomization of Newtonian Liquids in the Bag Breakup Regime: Comparison of Model Predictions to Experimental Data." *ICLASS 2012, 12th International Conference on Liquid Atomization and Spray Systems, Heidelberg, Germany.* September, 2012.

[10] Hwang, S.S., Liu, Z., and Reitz, R.D. (1996). Breakup mechanisms and drag coefficients of high-speed vaporizing liquid drops. *Atomization and Sprays*, 6 (3), 353-376.

[11] Flock, A. (2011). *Wake dynamics during aerodynamic fragmentation of liquid drops*. (Diploma) Thesis. Karlsruhe, Germany: Karlsruhe Institute of Technology.